JMEPEG (1993) 2:225-234

Mössbauer Studies of Rare Earth-Iron Hydrides, Carbides, and Nitrides

D.H. Ryan, X. Chen, and Z. Altounian

The basic principles of Mössbauer spectroscopy are introduced in the context of magnetically ordered alloys. A description of fitting procedures is presented, emphasizing the use of information derived from other techniques and indicating reliability limits. Ways in which the local structural and magnetic information obtained from Mössbauer spectroscopy can be used to probe the effects of hydrogen, carbon, and nitrogen additions in R2Fe17 alloys are presented, as well as how to distinguish local and global changes. Even apparently large-scale effects, such as a change in the magnetic easy direction, are shown to have clear local signatures. A new hybrid carbonitride of the 2-17 alloy series is introduced, which combines superior magnetic properties with enhanced thermal stability. The coherent two-phase structure of this material, revealed by Mössbauer spectroscopy, is used to emphasize the different information obtained from local and bulk measurements.

Keywords

carbides, Mössbauer spectroscopy, nitrides, permanent magnets, rare-earth alloys, samarium alloys, yttrium alloys

1. Introduction

UNLIKE techniques used to obtain the bulk characteristics of magnetic materials (e.g., T_C, magnetization, coercivity), Mössbauer spectroscopy provides information on microscopic properties (e.g., site moments, magnetic easy direction). It can also be used to probe the effects of chemical substitutions at an atomic level, to identify components in multiphase systems, and can distinguish different chemical environments within an alloy. Mössbauer spectroscopy allows quantitative assays of mixtures, because the spectral area of each component is related to the amount present. Furthermore, the technique is isotope specific (not just chemically specific), and it can thus be used to follow isotopically labeled substitutions. The technique is rarely used in isolation, because most technologically important materials yield complex spectra that are difficult to interpret without additional structural information obtained from X-ray or neutron diffraction.

In this article, the experimental technique of Mössbauer spectroscopy is introduced, and the various nuclear interactions that may be used to obtain information about the local magnetic properties of a material are identified. A review of what has been learned about the new series of magnetic materials—$R_2Fe_{17}Z_{3-\delta}$ (Z = H, C, N ..., $\delta \sim 0.5$)—is presented and concludes with a description of the latest development in this series—a hybrid carbonitride $R_2Fe_{17}N_xC_y(x + y \sim 3)$, a coherent two-phase combination of the carbide and nitride that retains the advantages of both. This material will be used to emphasize the distinction between bulk and microscopic measurements.

D.H. Ryan, X. Chen, and **Z. Altounian,** Centre for the Physics of Materials and Department of Physics, McGill University, Montreal, Quebec, Canada.

The data presented are on two related systems, one with a magnetic rare earth (Sm), the other with a nonmagnetic rare earth (Y). Comparison between the two systems, which have quite different magnetic properties, is used to establish consistency and improve the reliability of the fits. Several extensive Mössbauer studies of the nitrides and carbides of R_2Fe_{17} have been published,[1-3] and the results presented here are in general agreement with those works.

2. Mössbauer Spectroscopy

Mössbauer spectroscopy uses the resonant absorption of γ-rays by a nucleus to probe the hyperfine splitting of nuclear energy levels and thus obtain information on the atomic environment of the nucleus. A spectrum is normally obtained by measuring the absorption of a beam of γ-rays by a sample as a function of the γ-ray energy. The source most commonly used consists of a few tens of milliCuries (~1 GBq in SI units) of ^{57}Co diffused into a thin Rh foil. The ^{57}Co decays with a half-life of 270 days to an excited state of ^{57}Fe, which subsequently emits the 14.4 keV γ-ray used in the experiment. Because the 14.4 keV γ-rays are not very penetrating, samples are generally prepared in the form of thin foils or layers of fine powders with thicknesses on the order of 50 mg/cm^2. The source is normally kept at room temperature, and the sample is placed in an oven or cryostat to vary its temperature.

If the energy of the γ-ray corresponds to an allowed transition of a ^{57}Fe nucleus in the sample, it may be absorbed; otherwise, it passes through and is detected. The process is similar to other spectroscopic techniques such as atomic absorption spectroscopy, except that nuclear rather than atomic transitions are used, and the linewidths are many orders of magnitude smaller ($<10^{-8}$ eV). Because it is impossible to adjust the energy of a nuclear decay, energy scanning is achieved by exploiting the Doppler effect:

$$E' = E\left(1 + \frac{v}{c}\right)$$

where v is the velocity of the source, and c is the speed of light. In this form, the observed linewidth of the ^{57}Fe transition is

~0.13 mm/s (half-width at half maximum intensity), and the range of energy shifts needed to span the hyperfine splittings encountered lies in the range of ±10 mm/s. Such velocities are normally achieved by using an electromechanical transducer—essentially a highly linear loudspeaker—and the transmitted intensity is plotted versus the velocity imparted to the source. Positive velocities correspond to the source approaching the sample.

Three hyperfine interactions between the nucleus and its surroundings may be measured. The first is due to variations in the *s*-electron density at the nucleus and leads to an overall shift in the center of the pattern. This isomer shift, often denoted δ or IS, is affected by the bonding between the iron atom and its neighbors and can be used, for example, to distinguish between Fe^{2+} and Fe^{3+} valence states in compounds. In the absence of other effects, a single absorption line is observed, as shown in Fig. 1 for a sample of stainless steel. The second interaction leads to a splitting of the spectrum into two lines, as shown in Fig. 1. This quadrupole splitting, often denoted Δ or QS, arises through a coupling between the quadrupole moment of the nucleus and a nonspherical charge distribution in its immediate vicinity. Two sources of such a distribution are an asymmetric distribution of neighbors in a material (shown for $ZnFe_2O_4$ in Fig. 1), or an unpaired electron on the parent atom, such as the sixth 3*d* electron on the Fe^{2+} ion (shown for $FeSO_4$ in Fig. 1). Changes in D reflect changes in the atomic environment. Strictly speaking, the electric field gradient that leads to Δ is a tensor; however, because only two lines are observed and most samples are powders, the directional information is generally lost, and only the magnitude is observed. The third, and most important interaction in magnetic materials, is the magnetic hyperfine field, B_{hf}, which splits the spectrum into six lines (shown for αFe in Fig. 1) and arises through a coupling between the nuclear and atomic magnetic moments. Although comparison between Mössbauer hyperfine fields and neutron scattering derived local moments shows that the general trends are similar, B_{hf} is not directly proportional to the local atomic moment, and consequently, a simple comparison is not possible. Three contributions to B_{hf} may be distinguished in a metallic environment:

$$B_{hf} = B_{cp} + B_{4s} + B_{orb}$$

B_{cp} is due to the polarization of the 1*s*, 2*s*, and 3*s* shells by the 3*d* moment and leads to a field of −11.3 T/μ_B proportional to the 3*d* moment.[4] B_{4s} contains both a positive contribution due to polarization of the atom 4*s* valence electrons and a negative contribution due to a transferred hyperfine field from interactions with neighboring atoms. B_{orb} is due to the orbital moment of the iron atom, typically 0.1 μ_B,[5] with a proportionality factor of +42 T/μ_B.[4,6] The actual contributions of the three effects will vary from site to site within a structure, and so comparisons with the results of neutron scattering or band structure calculations must be made with care. Recognition of these differences is now leading to the extension of some band structure calculations to obtain hyperfine fields as well as local moments so that a more detailed comparison with experimental results will be possible.

In most important magnetic alloys, all three interactions are present simultaneously. Because the isomer shift is a scalar effect and just moves the pattern as a unit, it can be treated separately. However, when both Δ and B_{hf} are present, the two effects must be solved for together. To first order, if the magnetic field is dominant, the presence of Δ in a magnetic pattern leads to some minor changes in line positions. However, there is one major difference. The value of Δ measured is now not equal to $|\vec{\Delta}|$, but is given by the projection of $\vec{\Delta}$ onto the direction of $\vec{B}_{hf}$ and may therefore be reduced. Indeed, if the two vectors are perpendicular, Δ is zero. The vectorial nature of the B_{hf} -Δ combination leads to another complication in many magnetic alloys. For certain magnetic easy directions, the projections of Δ onto the symmetry-related magnetization directions

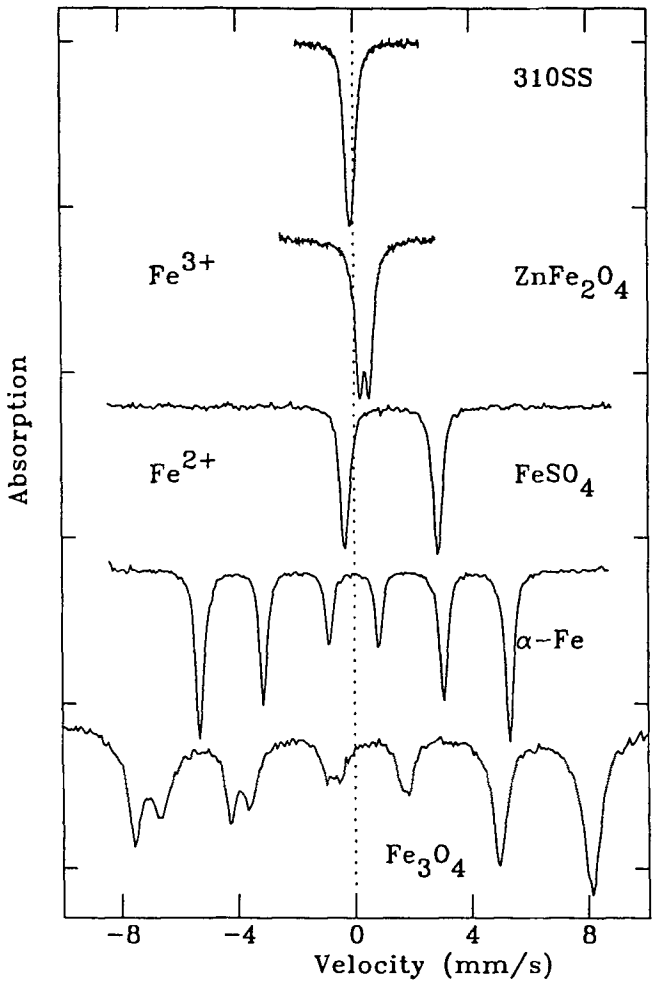

Fig. 1 Mössbauer spectra of some simple materials showing the effects of the three hyperfine interactions. Type 310 stainless steel (310SS) exhibits a single, sharp line displaced slightly negative from 0 mm/s by a small isomer shift. $ZnFe_2O_4$ exhibits a small quadrupole splitting due to an asymmetric arrangement of neighboring atoms. $FeSO_4$ exhibits a large quadrupole splitting due to an unpaired 3*d* electron on the Fe^{2+} ion. There is also a large positive isomer shift due to the very different electron densities in $FeSO_4$ and the iron metal used to set the zero isomer shift. Iron metal (αFe) exhibits a pure magnetic splitting of 33 T leading to a six-line spectrum. Magnetite (Fe_3O_4) has two distinct iron sites, and therefore, produces two overlapping six-line subspectra.

may not be equal, and this leads to a magnetic sub-splitting of the spectrum into two or more components with different values of Δ. Furthermore, the anisotropic contributions to B_{hf} can lead to the hyperfine fields for the sub-split contributions being different by a few Tesla.

Despite the apparent complexity indicated by the foregoing discussion, many spectra can be fitted directly, because enough of the components can often be identified visually to allow the parameters of any remaining sites to be determined from differences between the fit and the data. However, reliable fitting of the spectrum of a material with several crystallographically inequivalent sites, which are in turn magnetically sub-split, requires the use of information from other sources. The number of sites is normally taken from X-ray diffraction data. Some information on relative sizes of local moments often can be obtained from neutron diffraction. Magnetic easy directions, which control the number and intensity ratios of any sub-split components, can be obtained either from X-ray diffraction on magnetically aligned powders, or magnetization measurements on single crystals.

Even with extra information, it may not be possible to adequately resolve the spectral components, and some ambiguity often remains in the fit. Furthermore, the problem of assigning the various components to particular sites will remain. By far the most reliable guide to site assignments is intensity, and where possible, this will always be used first. Equal intensity sites can then be separated by moment size (either from neutron scattering or by estimation from the number of iron neighbors obtained from X-ray structure determinations), or by Δ, which will in general be smaller in symmetric sites than in highly distorted sites. However, the effect of the relative directions of the electric field gradient and magnetic easy direction must be included. Magnetically sub-split sites can be grouped according to known relationships between Δ for each sub-site; indeed, they are often fitted as a linked set. Where many sites of similar intensity are present, it may not be possible to identify all of the components uniquely, and several different combinations may fit the spectrum equally well. Average values will still be reliable; however, any interpretation that depends on detailed values should be treated with caution.

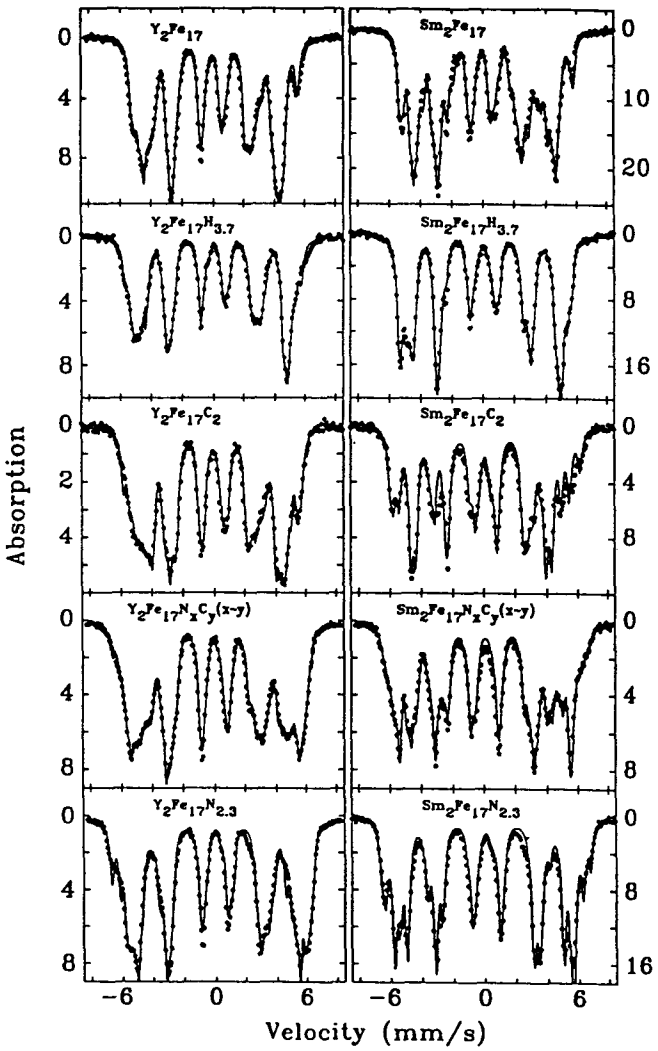

Fig. 2 Mössbauer spectra measured at 77 K for (top to bottom): $R_2Fe_{17}H_{3.7}$, R_2Fe_{17}, $R_2Fe_{17}C_2$, $R_2Fe_{17}N_xC_y$ ($x/y \sim 0.3$), and $R_2Fe_{17}N_{2.3}$. Data for R = Y are shown on the left and for R = Sm on the right.

2.1 R_2Fe_{17}

These compounds crystallize in two forms, with the early rare earths taking the rhombohedral $R\bar{3}m$ (Th_2Zn_{17}) form, and *Y* and the heavy rare earths (from Dy on) taking the hexagonal $P6_3/mmc$ (Th_2Ni_{17}) form. The two structures are closely related, and some of the R_2Fe_{17} compounds exist in both forms (e.g., Gd). In the rhombohedral case, there is a single rare earth site, 6*c*, whereas for the hexagonal structure, there are two occupied rare earth sites, (2*b*) and (2*d*). In both structures, there are four iron sites: 18*h*(12*k*), 18*f*(12*j*), 9*d*(6*g*), and 6*c*(4*f*), the notation being for the rhombohedral (hexagonal) forms, respectively. None of these compounds exhibits easy axis anisotropy at room temperature, although Tm_2Fe_{17} does so below 74 K.[7] The combination of easy-plane anisotropy and low ordering temperatures originally eliminated the 2-17 series alloys from consideration as potential permanent magnet compounds; however, the enhancements caused by light atom intercalation have revived interest.

Spectra measured at 77 K for the Sm and Y compounds are shown in Fig. 2. The easy magnetization direction lying in the basal plane causes a magnetic sub-splitting of the 18*h*(12*k*), 18*f*(12*j*), and 9*d*(6*g*) sites so that the spectra must be fitted with a total of eight subspectra in the ratio 12-6:6-6:6-3:6 (with sub-splittings denoted by the "-"). The presence of six equal intensity (6) components causes some ambiguity; however, the 6*c*(4*f*) site has the largest moment and is always well resolved, and the 18*f*(12*j*) group can be identified by their common isomer shift.

Fits (summarized in Table 1) yield closely similar hyperfine fields in each alloy, with the sequence $B_{hf}^{6c} > B_{hf}^{9d} > B_{hf}^{18f} > B_{hf}^{18h}$[8] in agreement with moment derived from neutron diffraction results on Nd_2Fe_{17}.[9] However, the neutron results do not fully distinguish the 9*d*, 18*f*, and 18*h* moments, and within error, all three moments are the same. The best consensus from spin-polarized band structure calculations yields $\mu^{6c} > \mu^{18f} > \mu^{18h} > \mu^{9d}$ (see Qi et al.[3] for a review of

Table 1 Hyperfine fields and isomer shifts of modified R_2Fe_{17} at 77 K

	6c(4f), T	9d(6g), T	18f(12j), T	18h(12k), T	⟨B_{hf}⟩, T	⟨IS⟩, mm/s
$Sm_2Fe_{17}H_{3.7}$	34.0	32.1	30.7	29.1	30.8	0.112
Sm_2Fe_{17}	34.5	29.3	25.8	25.3	27.3	0.017
$Sm_2Fe_{17}C_2$	37.6	33.2	27.9	25.7	29.2	0.026
$Sm_2Fe_{17}N_xC_y$ ($x < 0.5y$)	...	...	...	...	29.9	0.074
$Sm_2Fe_{17}N_xC_y$ ($x \sim y$)	...	...	...	...	31.6	0.117
$Sm_2Fe_{17}N_xC_y$ (sequential)	...	...	...	...	34.8	0.145
$Sm_2Fe_{17}N_{2.3}$	41.4	39.1	35.5	30.9	35.2	0.145
$Y_2Fe_{17}H_{3.7}$	35.5	31.6	30.8	28.5	30.7	0.097
Y_2Fe_{17}	32.1	29.7	26.8	26.2	27.7	0.006
$Y_2Fe_{17}C_2$	35.9	29.8	28.4	25.9	28.6	0.043
$Y_2Fe_{17}N_xC_y$ ($x < 0.5y$)	...	...	...	...	30.2	0.076
$Y_2Fe_{17}N_xC_y$ ($x \sim y$)	...	...	...	...	31.4	0.067
$Y_2Fe_{17}N_xC_y$ (sequential)	...	...	...	...	33.6	0.087
$Y_2Fe_{17}N_{2.3}$	40.1	35.3	34.9	31.4	34.3	0.084

this problem). Given the uncertain agreement between the Mössbauer and neutron results, it is not clear that the difference in sequence is significant. Assuming the calculations to be correct, one possible reason for the displacement of the 9*d* site may lie in the much shorter Fe-Fe distance compared with that for the 18*f* and 18*h* sites. This may lead to a larger B_{4s} contribution to B_{hf} at the 9*d* site and thus a larger total hyperfine field even though the contribution from the local 3*d* moment is smaller. Clearly, better neutron diffraction data are needed to confirm the moment sizes and check the calculations.

One distinctive feature of the 2-17 alloys is that, despite the large iron moments (~2.17 μ_B/Fe), they exhibit extremely low ordering temperatures, typically around room temperature, with only the Gd compound approaching 500 K. The compounds on either side of them in the phase diagrams (αFe on one side and either RFe_2 or R_6Fe_{23} on the other) have substantially higher ordering temperatures. The main reason is the weak exchange coupling associated with the very short Fe-Fe bonds on the 6*c* sites, which at 0.24 nm are close to the separation at which the Fe-Fe exchange interaction changes sign. Earlier high-pressure work showed a remarkably large pressure derivative of T_c in Y_2Fe_{17} (10 K/kbar[10]) and that change in T_c induced by hydriding followed the pressure derivative of T_c for all of the Y-Fe intermetallic compounds.[11] These results led to the expectation that any dilation of the lattice would raise T_c; H, C, and N have all been shown to have this effect.

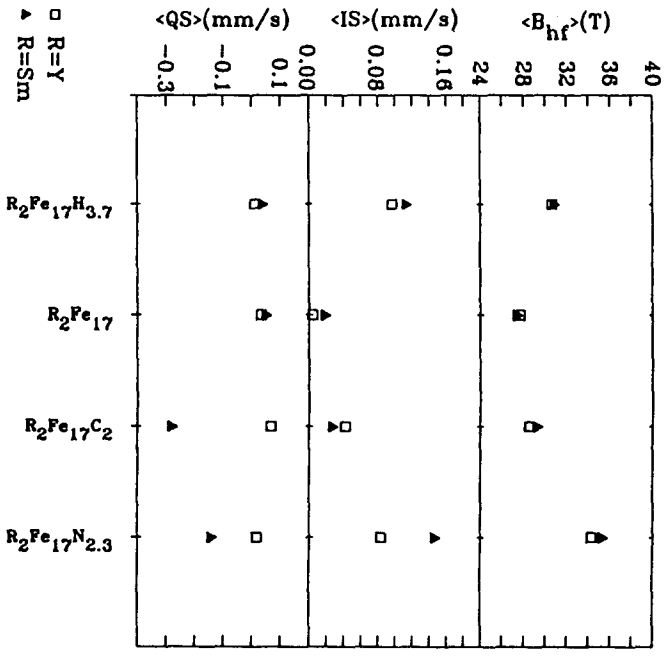

Fig. 3 Average values of the hyperfine field (⟨B_{hf}⟩) isomer shift (⟨IS⟩), and quadrupole splitting (⟨QS⟩) for the hydrides, carbides, and nitrides of the 2-17 alloys compared with the values in the starting materials. Measured at 77 K.

2.2 *R_2Fe_{17} Hydrides*

Hydrogen is by far the easiest interstitial to introduce. Annealing in 1 bar of H_2 at 250 °C is sufficient to give a hydrogen content of ~3 per formula unit and raise T_c (for the Sm compound) from 368 to ~500 K. The maximum T_c observable is limited by the tendency for the hydrogen to desorb;[12] indeed, the entire hydriding process is completely reversible, because the hydrogen may be extracted by raising the temperature and evacuating the chamber. Hydrogen has a strong affinity for the rare earths and essentially none for iron and, therefore, will tend to occupy sites of high rare earth coordination. Several suitable sites exist with two rare earth and 2-4 iron neighbors. A combined X-ray diffraction and Mössbauer study favored occupation of the 3*b* and 18*h* sites.[12] However, the close proximity of pairs of 18*h* sites means that only one of each pair can be occupied by hydrogen, and the other is then excluded.[13,14] This leads to a maximum hydrogen content of $R_2Fe_{17}H_4$, although higher values were claimed. A more recent neutron diffraction study of $Nd_2Fe_{17}D_x$ favored occupation of the 9*e* (the site also occupied by nitrogen and carbon, see below) and 18*g* sites, suggesting a maximum possible content of $x = 9$. However, the 18*g* sites form hexagonal rings in the *ab*-plane with *H-H* distances that are too short to allow full occupation, and only one-third occupation of the 18*g* site is possible, as was observed, leading to a total hydrogen content of $x \sim 5$. It is interesting to note that the 18*h* and 9*e* sites, distinguished in the two studies discussed above, are closely related (the 18*h* sites are reached through small displacements along the *c*-axis above

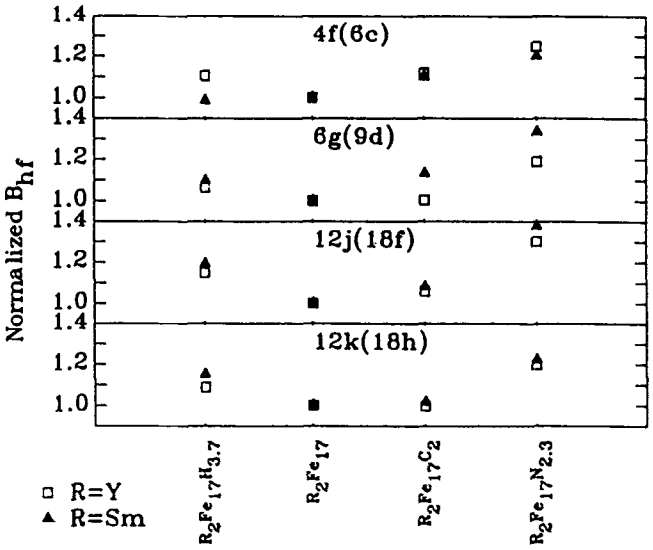

Fig. 4 Changes in the hyperfine field at each of the four crystallographically inequivalent sites in $R_2Fe_{17}Z_{3-\delta}$ (Z = H, C, N) normalized to the values in the starting alloy. Measured at 77 K.

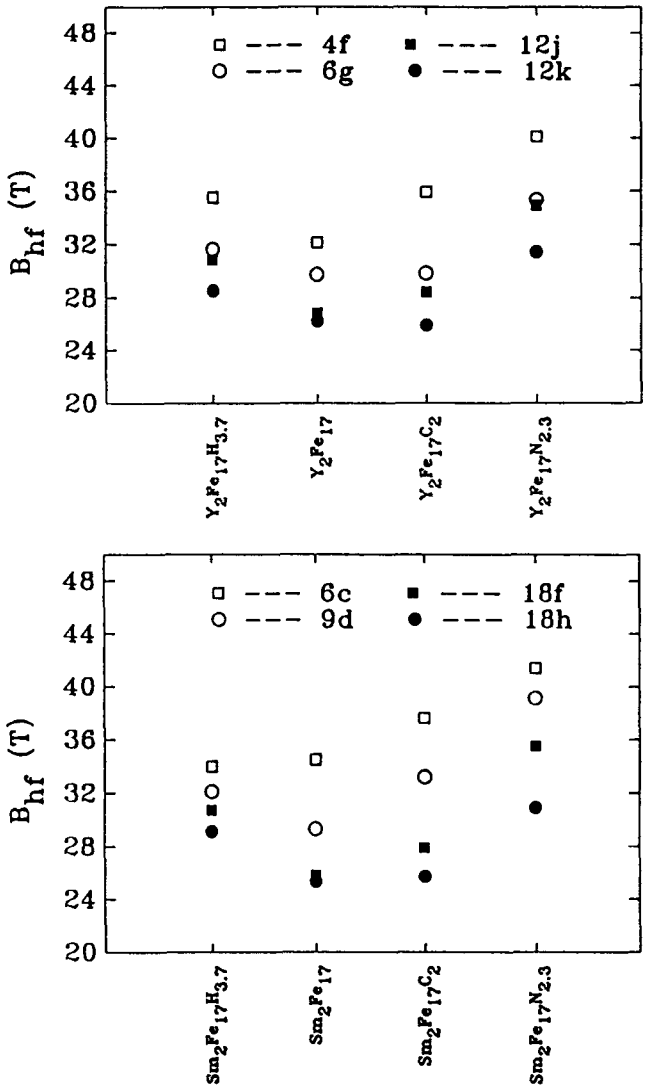

Fig. 5 Values of the hyperfine fields at each of the four crystallographically inequivalent sites in $R_2Fe_{17}Z_{3-\delta}$ (Z = H, C, N). Measured at 77 K.

and below each 9*e* site), and a regular 50% occupation of 18*h* is almost equivalent to full occupation of the 9*e* site.

Hydriding leads to large changes in the Mössbauer spectra of both the Y and Sm compounds, as shown in Fig. 2 and 3 and summarized in Table 1: A 12% increase in average hyperfine field and a 0.09 mm/s increase in average isomer shift (due mainly to the lattice expansion), whereas the average quadrupole splitting is essentially unchanged. The lack of change in $\langle\Delta\rangle$ is consistent with the X-ray diffraction observation of no crystal structure change and also indicates that the magnetic easy direction remains in the basal plane, which means that these alloys, although exhibiting improved magnetization and ordering temperature, are still unsuitable for permanent magnetic applications. However, from the Mössbauer point of view, the key feature of the hydrogen sites is that they only have 18*f* and 18*h* iron neighbors,[15] and thus, only these sites should be directly affected by the hydrogen. Indeed, the hyperfine field at both these sites increases by almost 20% (Fig. 4 and 5), whereas the change at the 9*d* site is closer to 10%. The 6*c* site in the Sm compound is slightly reduced (1%), whereas in the Y compound there is a 10% increase. This suggests that the lattice expansion alone leads to a 10% increase in iron moments, whereas having hydrogen neighbors yields an additional 10% increase. The origin of the difference in behavior at the 6*c* sites in the Y and Sm compounds is unclear.

The behavior of the isomer shift at each site on hydriding is more complex, although the trends are consistent between the Y and Sm compounds (Fig. 6). Both the 18*h* and 18*f* sites exhibit modest increases, whereas at the 6*c* site, there is a slight decrease, and the 9*d* exhibits a very large increase. The average behavior of δ (noted above and shown in Fig. 3) largely reflects the lattice expansion; however, the detailed behavior at each site also includes the effects of changes in bonding and electron transfer caused by the hydrogen, and no simple interpretation is possible. A sufficiently accurate band structure calculation to predict such changes is still not possible.

The site occupation of hydrogen, which is set largely by its strong affinity for the rare earth, places it in direct contact with only two of the four iron sites, and these two sites exhibit the largest change in hyperfine field and an increase in isomer shift, confirming the proximity of the hydrogen.

2.3 *R_2Fe_{17} Carbides and Nitrides*

Hydriding only raises the ordering temperature without inducing uniaxial anisotropy, and the hydrogen is easily removed by heating. As a result, the hydrides are not useful candidates for permanent magnets; however, the principle of intercalation modified magnetic materials is established, and other small atoms can be expected to have similar effects and to be more stable.

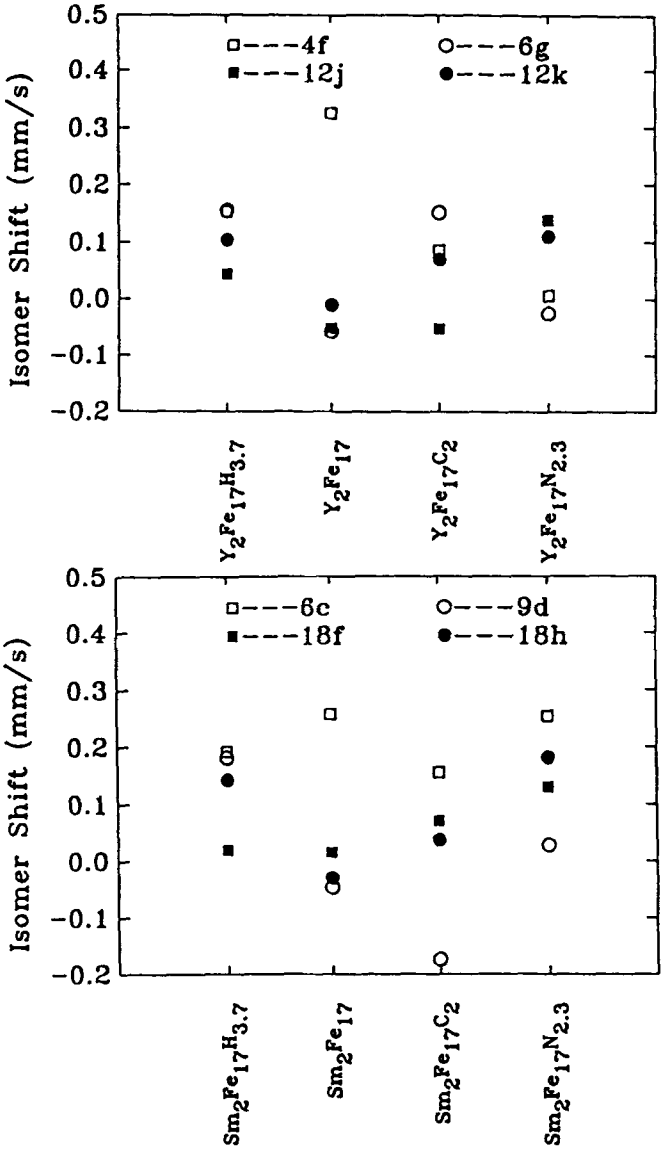

Fig. 6 Values of the isomer shift at each of the four crystallographically inequivalent sites in $R_2Fe_{17}Z_{3-\delta}$ (Z = H, C, N). Measured at 77 K.

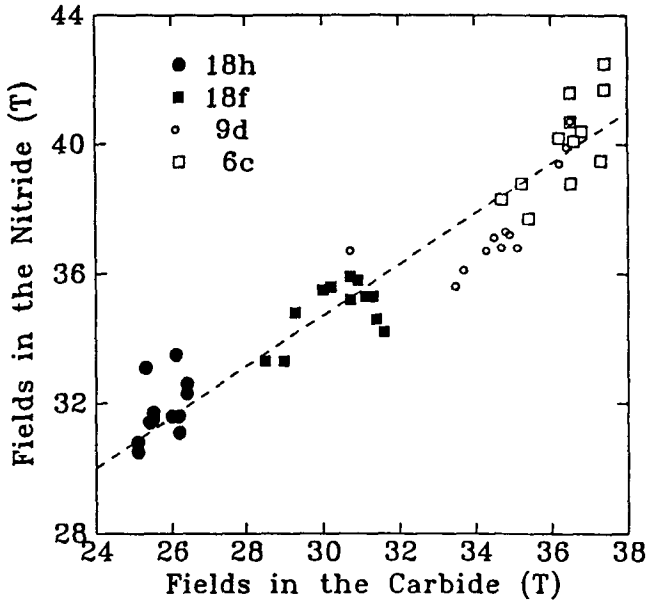

Fig. 7 Comparison among hyperfine fields at the four crystallographically inequivalent sites in $R_2Fe_{17}Z_{3-\delta}$ (Z = C, N) at 15 K. The correlation is essentially linear (dashed line), with no evidence of strong local effects of nitrogen or carbon coordination. Data taken from Qi et al.[2] and Hu et al.[1]

Carbon was the next element tried. The initial motivation was actually to replace the boron in $Nd_2Fe_{14}B$ to reduce the cost of the alloy. Such substitutions are possible, and the $R_2Fe_{14}C$ compounds are stable,[10] with the same crystal and magnetic structures as the parent borides.[16,17] However, there is a 10% reduction in T_c and a 6% reduction in iron moment on substituting carbon for boron in the Dy[18] and Lu[19] compounds. Later analysis showed that $R_2Fe_{17}C_x$ was also present and could be prepared as a single-phase alloy,[17,20] with $x \sim 1$ and with T_c increased by about 100 K compared with the parent R_2Fe_{17}. X-ray diffraction studies showed that the alloy retained the 2-17 structure and that the carbon occupied the 9*e* site.[17,21] However, the occupation is partial, and the thermal stability of the alloys appears to limit the carbon concentration to $x < 1.5$,[20,22,23] well below the maximum possible value of 3. Following the discovery that it was possible to introduce nitrogen by gas-solid reaction,[24,25] it was also demonstrated that 2-17 carbides with $x \sim 3$ could be prepared by the same route.[26,27] More recently, an alloy ($Sm_2Fe_{17}N_{5.2}$) has been prepared by annealing in 100 bar of N_2 at 823 K.[28] Both the carbides and nitrides have greatly enhanced T_c values of around 700 K, largely independent of the rare earth used,[2,29-31] indicating that the iron sublattice dominates the magnetic ordering. EXAFS measurements using the Sm L_{III} edge gave a N-Sm distance of 0.25 nm, suggesting that nitrogen, like carbon, occupied the 9*e* site.[32] Subsequent neutron scattering[33-35] and EXAFS measurements[36] confirmed this assignment. Little magnetic information is available from the neutron scattering measurements, because refinements were either done with a single iron moment[35] or with only the much larger 6*c* moment allowed to differ.[34]

Inspection of the Mössbauer spectra of the nitrides and carbides shown in Fig. 2 indicates that the iron moment in the carbides is significantly smaller than in the nitrides, or even in the hydrides. This may in part be due to the lower carbon contents ($x = 2$) compared with either the hydrides ($x = 3.7$) or nitrides ($x = 2.3$), but also results from a greater hybridization with the iron 3*d* orbitals in the case of carbon.[3] Table 1 and Fig. 3 show that the increase in $\langle B_{hf} \rangle$ in the case of carbon is quite modest (7% compared with 25% in the case of nitrogen), despite the fact that the ordering temperatures of the alloys are quite similar (688 K compared with 694 K for the carbide and nitride of the Y compound).

The average isomer shift (Fig. 3) shows the same positive trend observed in the hydrides, with the nitrides more positive than the carbides. However, the average quadrupole splitting exhibits a spectacular feature. Although the values for the Y

compounds are essentially unchanged, as would be expected with no change in crystal structure, those for the Sm compound show a pronounced (–0.2 mm/s) drop. A change in magnetic easy direction is the only possible cause, and this is confirmed to be easy-axis by X-ray diffraction on aligned powders.[25] Only the Sm compounds exhibit easy-axis anisotropy at room temperature, although the nitrides of the Er and Tm compounds do re-orient at 120 and 200 K, respectively,[30,37,38] and the carbides of the same parent compounds re-orient at 125 and 225 K, respectively.[2]

Despite the fact that C and N appear to occupy the same 9*e* site used by H, and the induced lattice expansions and T_c increases are similar, their effects on the neighboring iron moments are quite different. All of the hyperfine fields increase by about 20% in the nitrides, with only a slightly greater increase in the 18*f*, which has an N neighbor (Fig. 4). On the other hand, the carbides show only modest increases of ~10%, with the smallest changes at the 18*f* and 18*h* sites that have C neighbors (Table 1 shows that in the carbide of the Y compound B_{hf} actually decreases slightly at the 18*h* sites). Clearly, the effects of Fe-C bonding substantially reduce the gains associated with the lattice expansion, and the carbides are likely to be less technologically attractive than the nitrides. These trends are similar to those observed on substituting C for B in the $R_2Fe_{14}B$ alloy series discussed above. However, a comparison of the iron moments at the six crystallographically inequivalent sites in the $R_2Fe_{14}B$ and $R_2Fe_{14}C$ alloys showed a simple linear correlation between the boride and carbide moments, with no evidence of any local effects due to the nearest neighbor carbon atoms.[39] Similarly, a comparison of the carbides and nitrides of the R_2Fe_{17} alloys (Fig. 7), although exhibiting more scatter, shows essentially the same behavior. No local effects due to carbon coordination are apparent, although it is clear that the carbides have substantially smaller moments.

The very great chemical differences between C and N mean that band structure calculations, which only include the effects of lattice dilation,[40] will miss critical details, and the only other calculation to date[41] fails to reproduce the trends in the hyperfine field increases in $Y_2Fe_{17}N_3$, i.e., $\Delta B_{hf}^{12j} > \Delta B_{hf}^{4f} > \Delta B_{hf}^{12k} > \Delta B_{hf}^{6g}$ and actually predicts a reduction in the 12*j* site moment on nitriding. As the calculations give moments rather than B_{hf}, comparisons with the Mössbauer data are difficult, and thus far neither neutron scattering moments nor calculations of hyperfine fields are available.

2.4 R_2Fe_{17} Carbonitrides

Because carbon and nitrogen occupy the same site in the 2-17 structure and only one third occupancy can be achieved by alloying directly with carbon, it was natural to try filling the remaining 9*e* sites with nitrogen by annealing the alloy-formed carbide in nitrogen gas.[42] Such combined substitutions lead to alloys with increased T_c values (compared to the carbide alone), and the final value in the fully nitrided alloys appeared to be independent of the initial carbon content. However, the nitrided carbides were unstable, losing nitrogen above 560 K and decomposing fully to RN, RC, and αFe at 940 K. No Mössbauer data are available so far on these materials.

The authors have developed an alternative method for preparing carbonitrides of the R_2Fe_{17} compounds by dual gas-solid reactions. These may be carried out either simultaneously, by combining the nitrogen and hydrocarbon gases in the reaction chamber, or sequentially by reacting first with nitrogen, then with the hydrocarbon. Similar results are obtained in either case. The ordering temperatures obtained depend on the C:N ratio in the alloy (which is in turn controlled by the gas mixture used in the reaction) and interpolate between the pure carbide and pure nitride values.[43] X-ray diffraction yields sharp reflections showing that the parent structure is retained and that the alloy is uniform, and a single, sharp magnetic transition is observed at a temperature between those corresponding to the pure nitride and carbide (Fig. 8).

By contrast, the Mössbauer spectra of the Y-based and Sm-based carbonitrides in Fig. 2 show a very different picture. It is not possible to fit any of the carbonitride spectra using the standard sub-splitting into multiple sites, the reason being clear from a visual inspection. Consider the region of the Sm-carbonitride spectrum above 3 mm/s. The two strongest lines at ~3 and ~5.6 mm/s are distorted by the presence of precipitated αFe. Notice the feature just above 4 mm/s: this is clearly two lines and corresponds to a region in the nitride spectrum (shown below) that has no absorption lines. However, it does match the two-line feature in the carbide spectrum shown above. Similarly, there is broad absorption above 6 mm/s in the carbonitride that has a counterpart only in the nitride, not the carbide. The material is clearly some sort of mixture of the two phases. However, a simple-minded attempt to fit the carbonitride spectrum as a linear combination of the corresponding pure carbide and nitride spectra fails. It is necessary to allow the average hyperfine fields of the two components to vary, leading to a slight enhancement of $\langle B_{hf} \rangle$ in the carbide component and a similar reduction in the case of the nitride. The actual magnitude of these shifts depends on the relative proportions of the carbide and nitride phases in the alloy. Such a procedure reproduces the experimental pattern extremely well and yields parameters that differ only slightly from those used to fit the corresponding single intercalent alloy. One immediate result of this analysis is the C:N ratio present in the alloy, which can be compared with that in the gas mixture used in the reaction chamber. A consistent enrichment in nitrogen by almost a factor of two is observed, showing a strong preference for the nitrogen.

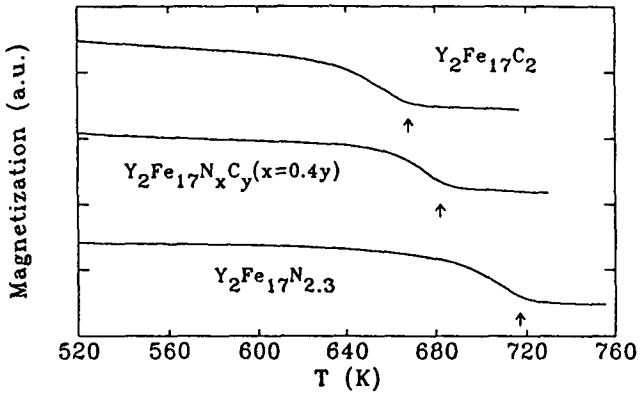

Fig. 8 Thermomagnetic scans for $Y_2Fe_{17}Z_{3-\delta}$ with Z = C, N_xC_y (x/y ~ 0.3), and N. Showing a single sharp T_c for the carbonitride that lies between the value for the pure nitride and carbide.

Two major questions are raised by this analysis: (1) How does the two-phase structure arise? (2) How can a clearly inhomogeneous alloy appear single phased to X-ray diffraction and magnetic measurements? Clearly, for such a structure to arise, there must be a strong tendency for C and N to avoid being in the same part of the alloy. This repulsion may in part be responsible for the instability of the nitrided carbide alloys noted above.[42] During the gas-solid reaction, the two elements diffuse into the alloy simultaneously. Once each has nucleated a region in a given grain, the other will be excluded from the vicinity and thus carbon-rich and nitrogen-rich regions will develop. These will then grow as the reaction proceeds until their boundaries meet. It is reasonable to expect that a given grain may have several nitride and carbide islands within it; indeed, to explain the X-ray diffraction and T_c behavior, multi-island grains are essential. This model is a variation on the shell model proposed by Coey et al. to explain how partially nitrided particles can exhibit a single magnetic transition.[44] Because the difference in lattice parameters between the pure nitride and pure carbide is on the order of 01.%,[43] they could easily grow coherently with a single, average lattice parameter controlled by the proportions of the two phases present. A lower limit on the island size can be obtained by noting that the lines in the Mössbauer spectra are quite sharp, meaning that the contribution from iron atoms on the boundaries between islands is relatively small, suggesting a minimum island length of ~100 nm (~1% of the atoms on the surface). The lattice mismatch is sufficiently small that coherent growth over many microns may be possible.

3. Conclusions

Mössbauer spectroscopy can be used to obtain detailed local information about magnetic ordering in alloys. As a local structural probe, it provides information that is complementary to the results of bulk measurements such as X-ray diffraction and magnetization. The microscopic information provided may be used to check the results of band structure calculations and also allows comparisons on a local level between a wide variety of magnetic alloys. In some special cases, the particular sensitivity of the technique is essential to understand the structure and composition of a material.

The carbonitrides demonstrate that it is possible to form a material that appears uniform both magnetically and structurally and yet clearly consists of a two-phase mixture. The site-specific microscopic information obtained from Mössbauer spectroscopy allows the two components to be identified and their relative proportions to be determined.

Acknowledgments

This research was supported by grants from the Natural Sciences and Engineering Research Council of Canada, Fonds pour la Formation de Chercheurs et l'aide à la Recherche, Québec, and Martinex Science Inc.

References

1. B.P. Hu, H.S. Li, H. Sun, and J.M.D. Coey, *J. Phys. Condens. Matt.*, Vol 3, 1991, p 3983
2. Q. Qi, H. Sun, and J.M.D. Coey, *Hyp. Int.*, Vol 68, 1991, p 27
3. Q. Qi, H. Sun, R. Skomski, and J.M.D. Coey, *Phys. Rev. B*, Vol 45, 1992, p 12278
4. R. Coehoorn, C.J.M. Denissen, and R. Eppenga, *J. Appl. Phys.*, Vol 69, 1991, p 6222
5. O. Eriksson, B. Johansson, R.C. Albers, A.M. Boring, and M.S.S. Brooks, *Phys. Rev. B*, Vol 42, 1990, p 2707
6. H. Ebert, P. Strange, and B.L. Gyorffy, *J. Phys. F*, Vol 18, 1988, p L135
7. P.C.M. Gubbens, A.M. van der Kraan, T.H. Jacobs, and K.H.J. Buschow, *J. Magn. Magn. Mater.*, Vol 80, 1989, p 265
8. B.P. Hu and J.M.D. Coey, *J. Less-Common Met.* Vol 171, 1991, p 33
9. J.F. Herbst, J.J. Croat, R.W. Lee, and W.B. Yelon, *J. Appl. Phys.*, Vol 53, 1982, p 250
10. K.H.J. Buschow, *Rep. Prog. Phys.*, Vol 54, 1991, p 1123
11. K.H.J. Buschow, *Solid State Commun.*, Vol 19, 1976, p 421
12. B. Rupp and G. Wiesinger, *J. Magn. Magn. Mater.*, Vol 71, 1988, p 269
13. D.G. Westlake, *J. Less-Common Met.*, Vol 90, 1983, p 251
14. D.G. Westlake, *J. Less-Common Met.*, Vol 91, 1983, p 1
15. O. Isnard, S. Miraglia, J.L. Soubeyroux, and D. Fruchart, *J. Less-Common Met.*, Vol 162, 1990, p 273
16. R.B. Helmholdt and K.H.J. Buschow, *J. Less-Common Met.*, Vol 144, 1988, p L33
17. D.B. de Mooij and K.H.J. Buschow, *J. Less-Common Met.*, Vol 142, 1988, p 349
18. P. Deppe, M. Rosenberg, and H.H. Stadelmaier, *J. Less-Common Met.*, Vol 143, 1988, p 77
19. C.J.M. Denissen, D.B. de Mooij and K.H.J. Buschow, *J. Less-Common Met.*, Vol 139, 1988, p 291
20. X.P. Zhong, R.J. Radwanski, F.R. de Boer, T.H. Jacobs, and K.H.J. Buschow, *J. Magn. Magn. Mater.*, Vol 86, 1990, p 333
21. G. Block and W. Jeitschko, *Inorg. Chem.*, Vol 25, 1986, p 279
22. W.G. Haije, T.H. Jacobs, and K.H.J. Buschow, *J. Less-Common Met.*, Vol 163, 1990, p 353
23. J. Ding and M. Rosenberg, *J. Less-Common Met.*, Vol 166, 1990, p 313
24. J.M.D. Coey and H. Sun, *J. Magn. Magn. Mater.*, Vol 87, 1990, p L251
25. H. Sun, J.M.D. Coey, Y. Otani, and D.P.F. Hurley, *J. Phys. Condens. Matt.*, Vol 2, 1990, p 6465
26. J.M.D. Coey, H. Sun, Y. Otani, and D.P.F. Hurley, *J. Magn. Magn. Mater.*, Vol 98, 1991, p 76
27. H. Sun, Y. Otani, and J.M.D. Coey, *J. Magn. Magn. Mater.*, Vol 104-7, 1992, p 1439
28. H. Uchida, H.H. Uchida, T. Yanagisawa, H. Kaneko, U. Koike, K. Kamada, Y. Matsumara, T. Noguchi, and T. Kurino, *J. Alloys Comp.*, Vol 184, 1992, p L5
29. K.H.J. Buschow, R. Coehoorn, D.B. de Mooij, K. de Waard, and T.H. Jacobs, *J. Magn. Magn. Mater.*, Vol 92, 1990, p L35
30. Y. Otani, D.P.F. Hurley, H. Sun, and J.M.D. Coey, *J. Appl. Phys.*, Vol 69, 1991, p 5584
31. J.M.D. Coey, *Phys. Scr.*, Vol T39, 1991, p 21
32. J.M.D. Coey, J.F. Lawler, H. Sun, and J.E.M. Allan, *J. Appl. Phys.*, Vol 69, 1991, p 3007
33. R.M. Ibberson, O. Moze, T.H. Jacobs, and K.H.J. Buschow, *J. Phys. Condens. Mat.*, Vol 3, 1991, p 1219
34. S. Miraglia, J.L. Soubeyroux, C. Kolbeck, O. Isnard, D. Fruchart, and M. Guillot, *J. Less-Common Met.*, Vol 171, 1991, p 51
35. O. Isnard, S. Miraglia, J.L. Soubeyroux, D. Fruchart, and D. Pannetier, *Phys. Rev. B*, Vol 45, 1991, p 2920
36. T.W. Capehart, R.K. Mishra, and F.E. Pinkerton, *Appl. Phys. Lett.*, Vol 58, 1991, p 1395

37. B.P. Hu, H.S. Li, H. Sun, J.F. Lawler, and J.M.D. Coey, *Solid State Commun.*, Vol 76, 1990, p 587

38. P.C.M. Gubbens, A.A. Moolenaar, T.H. Jacobs, and K.H.J. Buschow, *J. Alloys Comp.*, Vol 176, 1991, p 115

39. G.L. Long, O.A. Pringle, G.K. Marasinghe, F. Grandjean, and K.H.J. Buschow, *J. Appl. Phys.*, Vol 69, 1991, p 6040

40. T. Beuerle, P. Braun, and M. Fähnle, *J. Magn. Magn. Mater.*, Vol 94, 1991, p L11

41. S.S. Jaswal, W.B. Yelon, G.C. Hadjipanayis, Y.Z. Wang, and D.J. Sellmyer, *Phys. Rev. Lett.*, Vol 67, 1991, p 644

42. X.C. Kou, R. Grössinger, M. Katter, J. Wecker, L. Schultz, T.H. Jacobs, and K.H.J. Buschow, *J. Appl. Phys.*, Vol 70, 1991, p 2272

43. Z. Altounian, X. Chen, L.X. Liao, D.H. Ryan, and J.O. Ström-Olsen, *J. Appl. Phys.*, Vol 73, 1993, in press

44. J.M.D. Coey and D.P.F. Hurley, *J. Magn. Magn. Mater.*, Vol 104-7, 1992, p 1098